



Modelling Storm-load Sediment Deposition Thresholds for Potential Ecological Effects in Okura Estuary

Karepiro Bay: Model Development and
Calibration

May

TR 2010/024

Reviewed by:

Approved for ARC Publication by:



Name: Megan Stewart

Name: Grant Barnes

Position: Project Leader – Marine

Position: Group Manager – Monitoring & Research

Organisation: Auckland Regional Council

Organisation: Auckland Regional Council

Date: May 2010

Date: May 2010

Recommended Citation:

Pritchard, M.; Reeve, G.; Swales, S. (2009). Modelling storm-load sediment deposition thresholds for potential ecological effects in Okura Estuary / Karepiro Bay: Model development and calibration. Prepared by Organisation for Auckland Regional Council. Auckland Regional Council TR2010/024.

© 2008 Auckland Regional Council

This publication is provided strictly subject to Auckland Regional Council's (ARC) copyright and other intellectual property rights (if any) in the publication. Users of the publication may only access, reproduce and use the publication, in a secure digital medium or hard copy, for responsible genuine non-commercial purposes relating to personal, public service or educational purposes, provided that the publication is only ever accurately reproduced and proper attribution of its source, publication date and authorship is attached to any use or reproduction. This publication must not be used in any way for any commercial purpose without the prior written consent of ARC. ARC does not give any warranty whatsoever, including without limitation, as to the availability, accuracy, completeness, currency or reliability of the information or data (including third party data) made available via the publication and expressly disclaim (to the maximum extent permitted in law) all liability for any damage or loss resulting from your use of, or reliance on the publication or the information and data provided via the publication. The publication and information and data contained within it are provided on an "as is" basis.

Modelling storm-load sediment deposition thresholds for potential ecological effects in Okura Estuary/Karepiro Bay: Model development and calibration

Mark Pritchard
Glen Reeve
Andrew Swales

Prepared for
Auckland Regional Council

NIWA Client Report: HAM2009-106
June 2009

NIWA Project: ARC09220

National Institute of Water & Atmospheric Research Ltd
Gate 10, Silverdale Road, Hamilton
PO Box 11115, Hamilton, New Zealand
Phone +64-7-856 7026, Fax +64-7-856 0151
www.niwa.co.nz

Contents

1	Executive Summary	1
2	Introduction and Rationale	3
2.1	Study aims	3
2.2	Rationale	4
2.3	Study site	6
2.4	Catchment scaling, sediment yields, and freshwater discharge	6
2.5	Wind conditions	9
2.6	Oceanographic data	10
2.7	Summary of methodology	12
3	Model Development, Setup and Calibration	13
3.1	Modelling overview	13
3.2	The MIKE3 FM HD and MT model	13
3.3	Model mesh development	14
3.4	Calibration parameters	17
3.5	Calibration data	17
3.6	Offshore tidal boundary conditions	18
3.7	Wind forcing	18
3.8	Calibration of water surface elevations	18
3.9	Calibration of currents	20
3.10	Salinity	23
3.11	MT sediment transport module calibration	26
3.12	Observations and MT module setup	26
4	MT Model Scenario Setup	30
5	Summary	31
6	Acknowledgements	32
7	References	33

8	Appendix 1: Formulation of processes simulated by the MIKE3 models	35
8.1	Bed shear stress	35
8.2	Currents	35
8.3	Salinity	36
8.4	Sediment transport	36
8.4.1	Deposition	36
8.4.2	Erosion	37
9	Appendix 2: LIDAR data processing	39

Reviewed by:



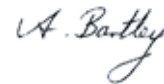
Scott Stephens

Approved for release by:



Dave Roper

Formatting checked



1 Executive Summary

Auckland Regional Council (ARC) commissioned the National Institute for Water and Atmospheric Research Ltd (NIWA) to develop a robust and scientifically defensible monitoring plan to assess the effects of harvesting the Weiti Forestry Block (WFB) at Okura, Northland, New Zealand. Deforestation through logging in the region has the potential of delivering elevated loads of fine sediments into local estuarine environments. The subsequent dispersal and deposition of fine sediments in the adjacent Okura and Weiti estuaries has a potential for detrimental ecological impacts on local benthic flora and fauna.

The effects of forest harvesting were to be investigated through a combination of data collection, data analysis and numerical modelling. Measurements of localised stream/river sediment yields, stream/river freshwater discharge rates, tidal and weather data were used to develop a numerical modelling protocol for the Okura Estuary and immediate receiving waters in Kaiparo Bay. The models used in the study were the DHI Water and Environment MIKE3 FM HD hydrodynamic model and the DHI MIKE3 FM MT (mud) sediment transport model,

The Okura Estuary model bathymetric mesh was produced from the combination of digitised admiralty charts, LIDAR surveys supplied by the ARC and a bathymetric survey by NIWA. The NIWA survey provided extra information on the intertidal mud flats and in the tidal creeks.

The implementation and calibration of the MIKE3 FM modules was based on two field data sets collected between October and December 2008. These time series of observed water levels, currents and suspended sediment concentrations were used to calibrate the model(s).

The calibrated hydrodynamic model provided good predictions of water surface elevations and semi-diurnal tidal currents.

The model was sourced with freshwater inputs from monitored and scaled catchment freshwater sources and provided a reasonable estimate of salinity in the Okura Estuary. This was important for predicting the dispersal of catchment-derived sediments due to freshwater runoff.

Measurements of suspended sediment concentration from two separate sites in the estuary were then used to calibrate the MIKE3 MT sediment transport model.

The model was configured to investigate the resuspension and transport of 15µm particles. The modelled constituent concentration was then compared to the measurements. The calibrated model was able to satisfactorily reproduce the phase and magnitude of suspended sediment concentration under multiple tide cycles, and under weak winds. However, the model was deficient in simulating some of the inherent variability of the region driven by wind wave re-suspension.

The calibrated model was ready for the next stage of the study where 36 different simulations with different combinations of sediment yield, river discharge, wind speed

and direction, and tidal range were to be used to produce a series of 'event' return time lookup tables. The lookup tables summarise the extent of sediment deposition based on a specific unique event. These tables would then be used to access the potential level of sedimentation at each site and help steer a management decision for the WFB based on local river discharges, and atmospheric and ocean forcing conditions.

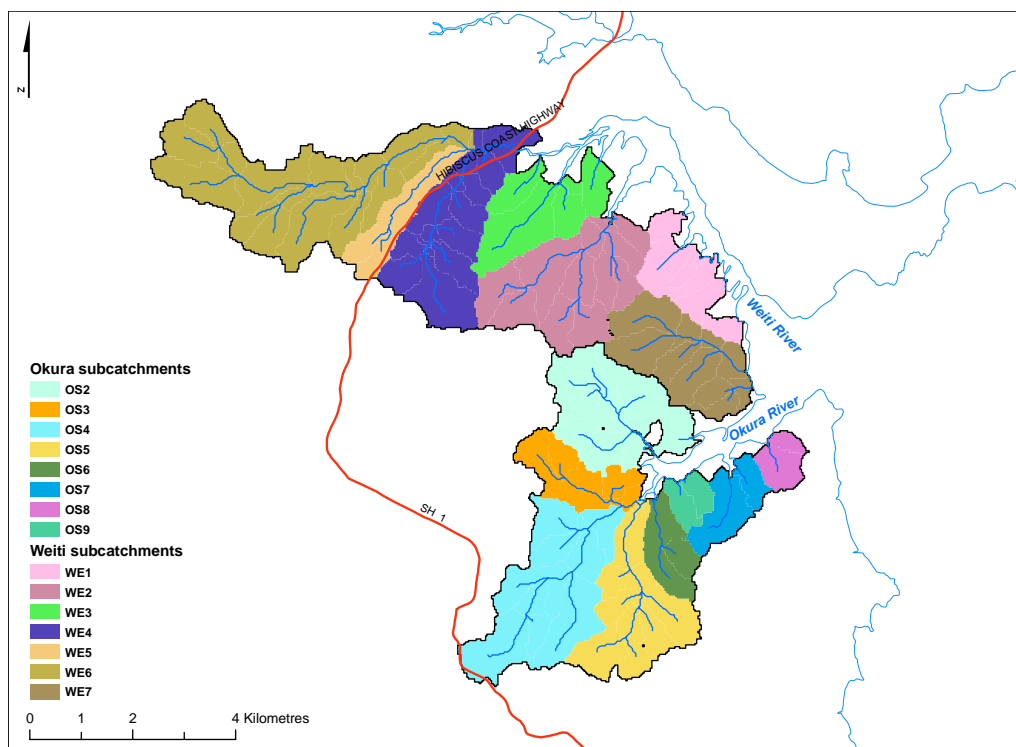
2 Introduction and Rationale

2.1 Study aims

The Auckland Regional Council (ARC) has identified that harvesting of the Weiti Forestry Block (WFB) at Okura has the potential for adverse environmental effects due to elevated levels of soil erosion through tree felling on receiving estuarine environments (see Figure 1). These potential adverse effects primarily relate to fine-sediment delivery, dispersal and deposition in the adjacent Okura and Weiti estuaries and resulting ecological impacts. The 8.8 km² WFB is planned to be harvested during the next five years.

Figure 1:

Regional schematic map of sub-catchments discharging to the Okura and Weiti Estuaries.



The ARC commissioned NIWA to develop a robust and scientifically defensible monitoring plan for the timely detection of adverse effects of eroded fine-sediments on benthic flora and fauna at specific sites in the receiving estuary waters during the harvesting of the WFB. The 'harvesting phase' includes the post-harvest period or the time period after logging operations have ceased and before the harvested area is fully

stabilised by re-vegetation or some alternative method that reduces soil erosion to near pre-harvest levels.

Figure 2 shows the location of 21-sample sites selected in agreement with the ARC. These were regions of immediate interest to the ARC as they identified areas of specific communities of flora and fauna which maybe stressed under increased levels of sedimentation.

This report covers the methodology plus development and calibration of a numerical hydrodynamic and sediment transport model of the Okura Estuary used to meet these aims.

2.2 Rationale

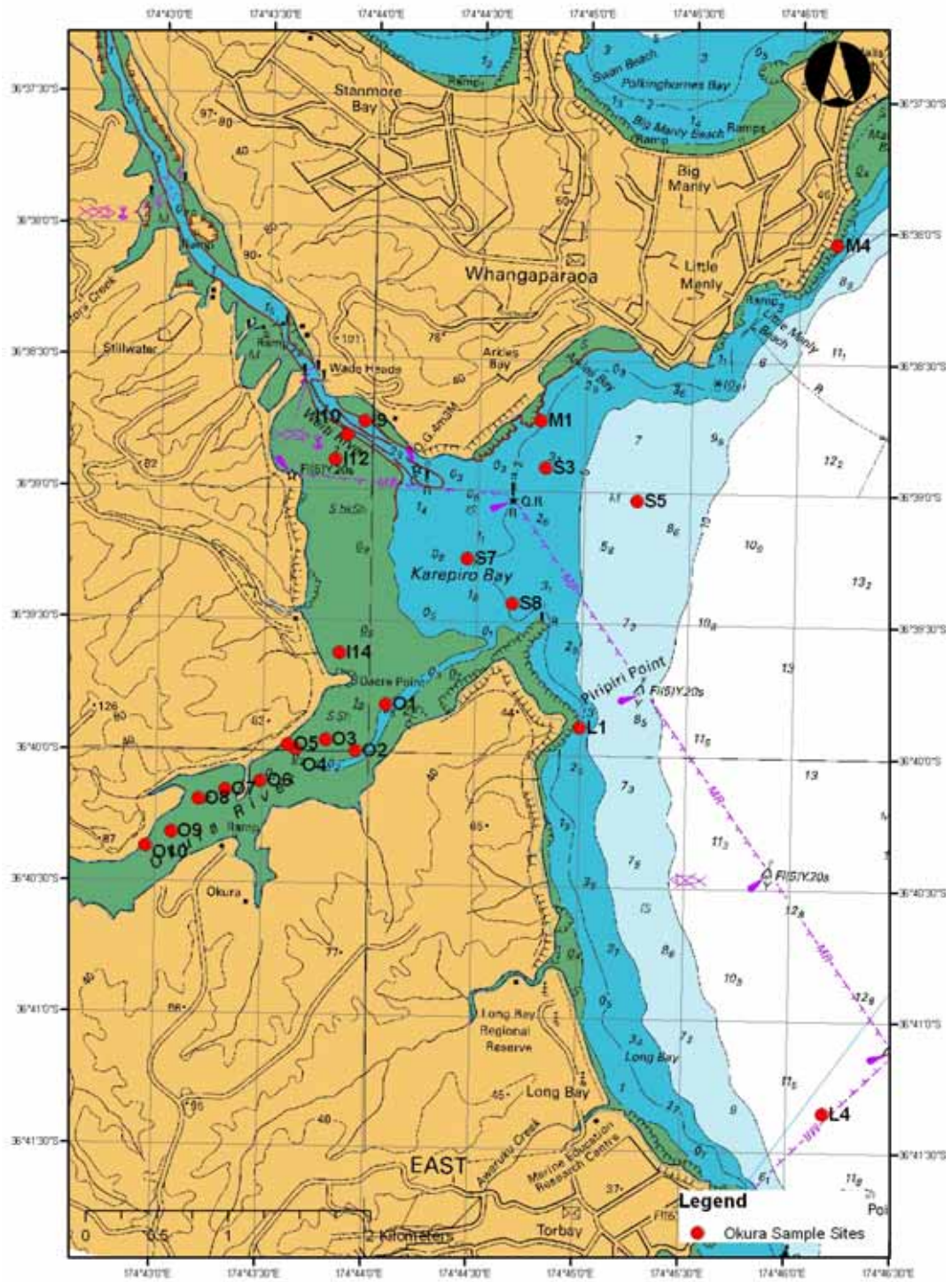
A 6.25-year time series of storm driven sediment yields and the associated river discharge into the Okura Estuary was used to estimate a specific sediment yield and storm river discharge rate for a range of 'event' return periods. The range of return periods extended from 1-month to 10-years to cover and slightly extrapolate on the measured range of return periods. These yields and discharges were then scaled to cover other unmonitored catchments in the region that also discharged into the Okura Estuary. Further analysis of wind speed and direction along with tidal data provided localised trends in atmospheric and ocean forcing. Therefore, in summary the events were classified on the basis of:

- Event yield and flow magnitude.
- Wind speed and direction.
- Tidal amplitude.

Based on the data analysis the DHI MIKE3 FM HD hydrodynamic and MT sediment transport modelling suite was forced with a specific unique combination of sediment yield, river discharge, wind and tide to produce a predicted level of sedimentation at a specific site of interest in the estuary (see Figure 2). The result of each event would then be incorporated into a series of 'lookup tables'. These tables based on a unique combination of event driven sediment yield, river discharge, wind speed and direction, and tidal range would then be used to access the potential level of sedimentation at each site and help steer a management decision for the WFB based on local river discharges, and atmospheric and ocean forcing conditions.

Figure 2:

Hydrographic chart (NZ5321) showing the location of the Okura Estuary and the sample sites selected for scenario driven sediment deposition.



2.3 Study site

The Okura Estuary has a high-tide surface area of 1.4 km², which is small in comparison to its 22.7 km² land catchment. Some 50% of the WFB is contained within the 4.6 km² North Branch sub-catchment, which discharges to the upper reaches of the Okura Estuary (Figure 1, OS-2). A further c. 3 km² of the Weiti Forestry Block (WFB) is contained in sub-catchment WE7, which discharges directly to Karepiro Bay immediately seaward of the Okura and Weiti Estuaries. Runoff from the remaining c. 1.2 km² of the WFB discharges to Weiti Estuary from sub-catchments WE1–WE3.

Okura Estuary shown in Figure 2 is c. 80% intertidal, with a single main tidal channel flanked on both sides by flats that are submerged to an average depth of one metre at high tide (Swales et al. 2002). Because the estuary is largely intertidal, there is almost complete exchange of estuarine water on each tide.

2.4 Catchment scaling, sediment yields, and freshwater discharge

Synthesised event driven sediment yields (Y) and average fresh water discharge (Q_{avg}) for the un-monitored catchments surrounding the Okura Estuary (OS2-OS9) and Karepiro Bay (WE7) were derived from a catchment area scaling analysis (see Figure 1). This employed the results from the earlier work of Hicks et al. (2009) and GIS catchment area maps.

OS4 (Awanohi) was used as the reference catchment as a continuous record of both sediment yield and freshwater runoff extended back in time some 6.25 years.

Table 1:

Catchment areas and scaling factors used in conjunction with sediment and flow data to produce catchment sediment yields and river and creek discharge rates for modelling study.

Catchment	Area (m ²)	Scale Factor
OS2	4587975	0.75
OS3	2141055	0.35
OS4	6117300	1
OS5	4159764	0.68
OS6	1468152	0.24
OS7	1529325	0.25
OS8	856422	0.14
OS9	734076	0.12
WE7	4159764	0.69

The Awanohi data was first scaled up by 8% to take into account the portion of the catchment area not captured by the monitoring station. Table 1 shows results from the final scaling analysis which tables the proportional area of each catchment with respect to that of OS4 based on the ratio:

$$Sf = Xa / OS4a$$

Where:

Xa=Area of catchment

OS4a= Area of OS4 catchment

Sf= Scale factor

Hicks et al. (2009) compared event sediment yields with peak discharge flows (Q_p). For the purpose of the present study, the event yield was compared to the average source freshwater discharge rate (Q_{avg}) computed from the catchment area, total event runoff, and quickflow period. This volume based analysis is idealised but for the purpose of running many numerical model scenarios, it was easier to implement in the MIKE3 FM model setup and also compare and contrast inter-scenario results.

Figure 3:

Event sediment yield (Y) for the Awanohi River with respect to return time period. Data modified after Hicks et al. (2009).

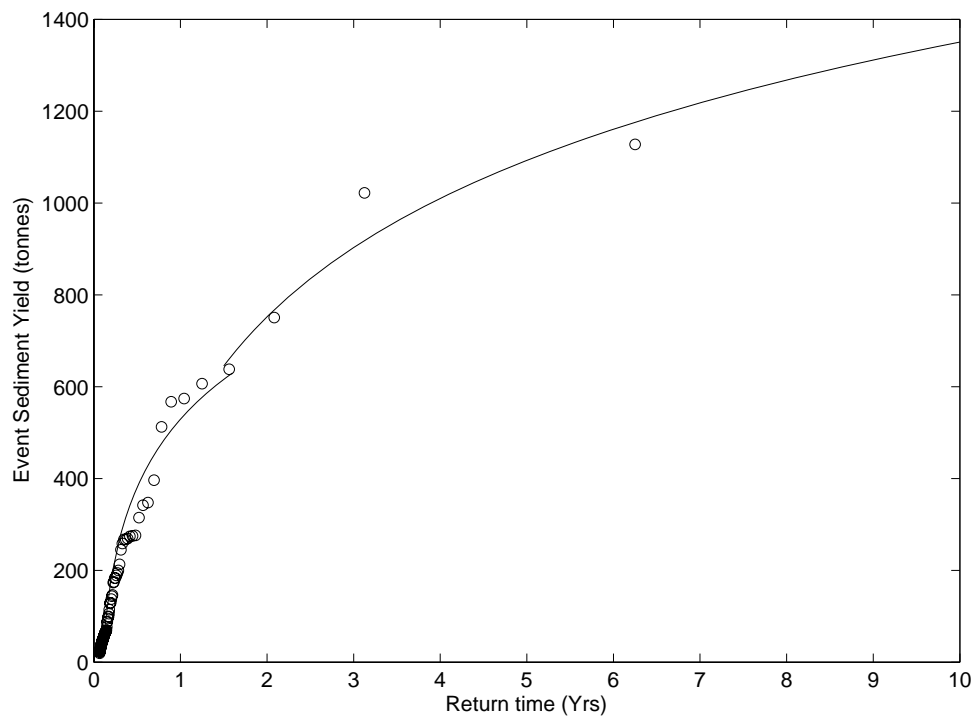


Figure 3 shows the Y frequency relations with respect to return time for the Awanohi (OS4) catchment based on return periods calculated by Hicks et al. (2009). Two separate lines of best natural log ($1/n$) fit are superimposed on the data. The lower bound fit extends from return times of 0 to 1.5 years and the higher from 1.5 to 10

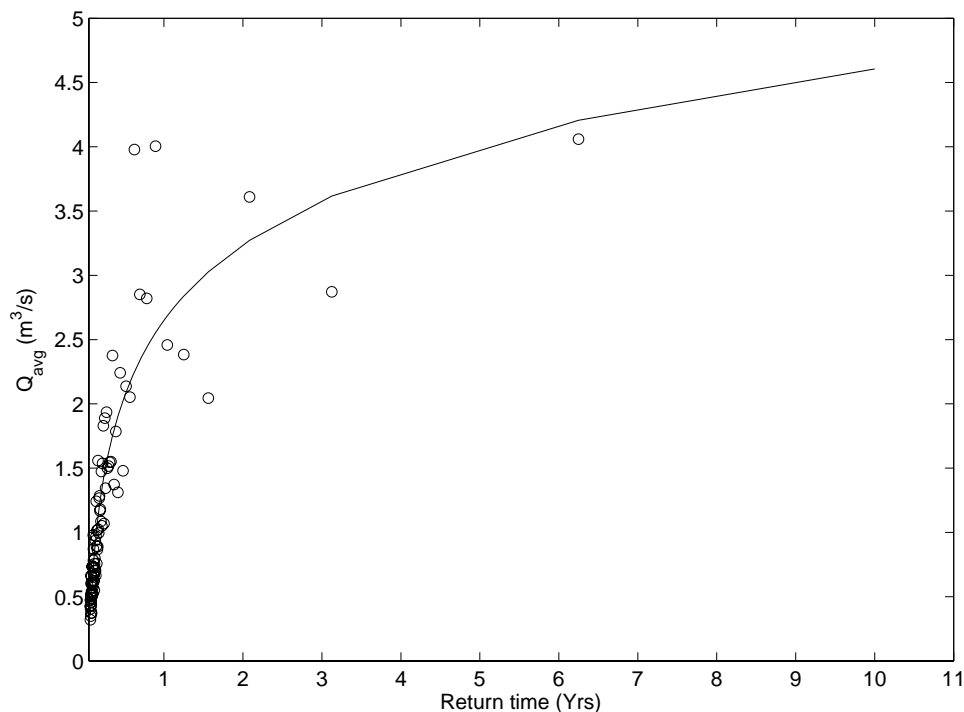
years. Both fits to the data have R^2 values of > 0.9 . Figure 4 shows the same range of Y return times to the corresponding value of Q_{avg} calculated from the catchment volumetric analysis. The line of best fit to the data had $R^2 > 0.9$.

From the data fits, event sediment loads and event average discharge rates for 1 month, 3 months, 1 year and 10 years Y return times were selected. This time span covered a range of potential input scenarios to the Okura estuary under varying flow conditions under a realistically predictable time frame i.e., based on the data.

The best fits and scaling factors shown in Table 1 were then used to estimate the Y and Q_{avg} for each of the catchments. The combined Y and Q_{avg} values for each of the selected return times for catchments OS3 to OS6 and OS7 to OS9 along with the predictions for OS2 and WE7 were then used to produce model sediment and freshwater inputs for 4-source inputs. More detail on model scenario inputs is given in later sections.

Figure 4:

Average river discharge rate (Q_{avg}) for the Awanohi River with respect to return time period. Data modified after Hicks et al. (2009).

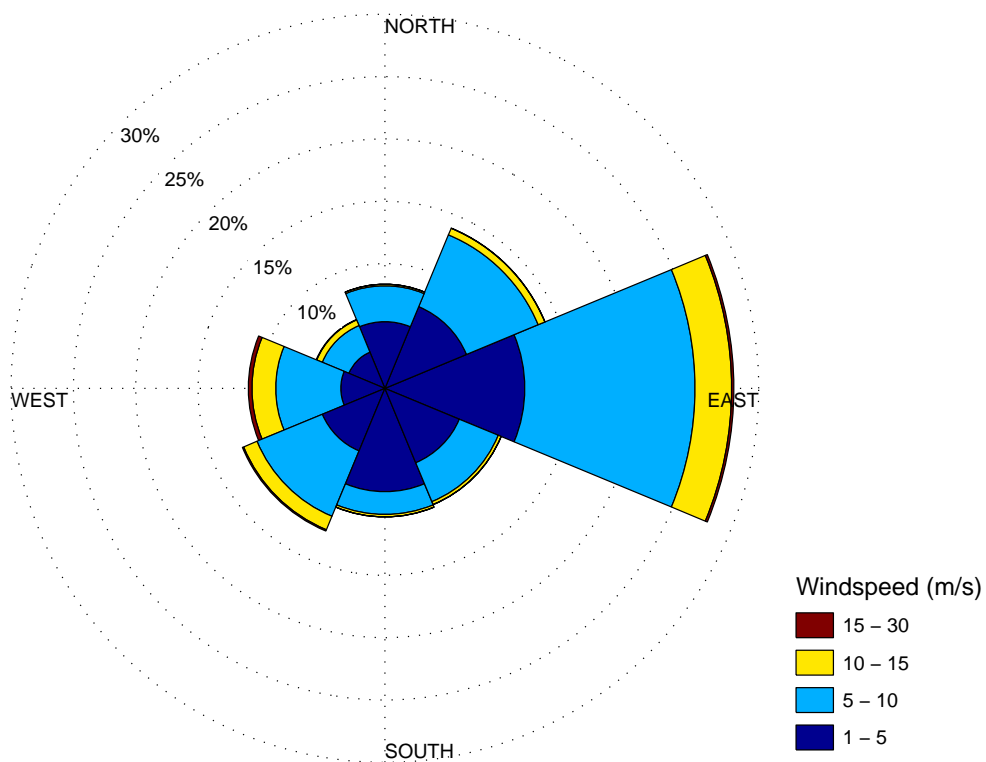


2.5 Wind conditions

Figure 5 presents the wind rose that describes a near 12 year continuous time series of wind speed and directional data recorded at Whangaparaoa airport between 1997 and 2009. Although the mean wind speed of 5.37 m/s was directed from the south (189 deg), the wind rose analysis shows both strong Easterly and Westerly winds. As the Okura is narrow, longitudinally aligned along a North-easterly – South-westerly axis and flanked to the north and south by a valley, only the impact of calm and bi-directional winds from the NE or SW are simulated in the model scenarios. A median wind speed of 7.5 m/s was applied in the model for all the scenarios that included localised wind driven effects. The median was selected on the basis that although mean winds were $O(5\text{ m/s})$, previous work has suggested winds below 7.5 m/s have little or no effect in the model.

Figure 5:

Wind rose describing wind speed and directional data recorded at Whangaparaoa between 1997 and 2009.



2.6 Oceanographic data

Oceanographic data comprising of: pressure (depth); optical backscatter (suspended sediment concentration), conductivity and temperature and profiles of water velocities were recorded at several sites in the Okura Estuary channel and in Karepiro Bay. Figure 6 shows the location of the mooring sites and Table 2 gives a brief summary of each moorings instrument type, deployment details, sample rate, and transducer (data) type.

Pressure transducer (PT) records from all sites were, by assuming the hydrostatic approximation converted to depth. OBS data was calibrated using sediment samples collected by each mooring. Conductivity and temperature (CT) data was converted to salinity for the three DOBIEs fitted with CT sensors (Fofonoff and Millard, 1983). The ADCP velocity data was corrected for local magnetic declination so currents were relative to true North.

These data are used through the report for both the calibration of the MIKE3 FM HD and MT models. The PT data recorded at the BND mooring site was subject to harmonic analysis and the semi-diurnal tidal constituents were eventually used to produce idealised tidal boundary conditions for specific tidal ranges used in the modelled scenarios and used to produce results for the final lookup tables.

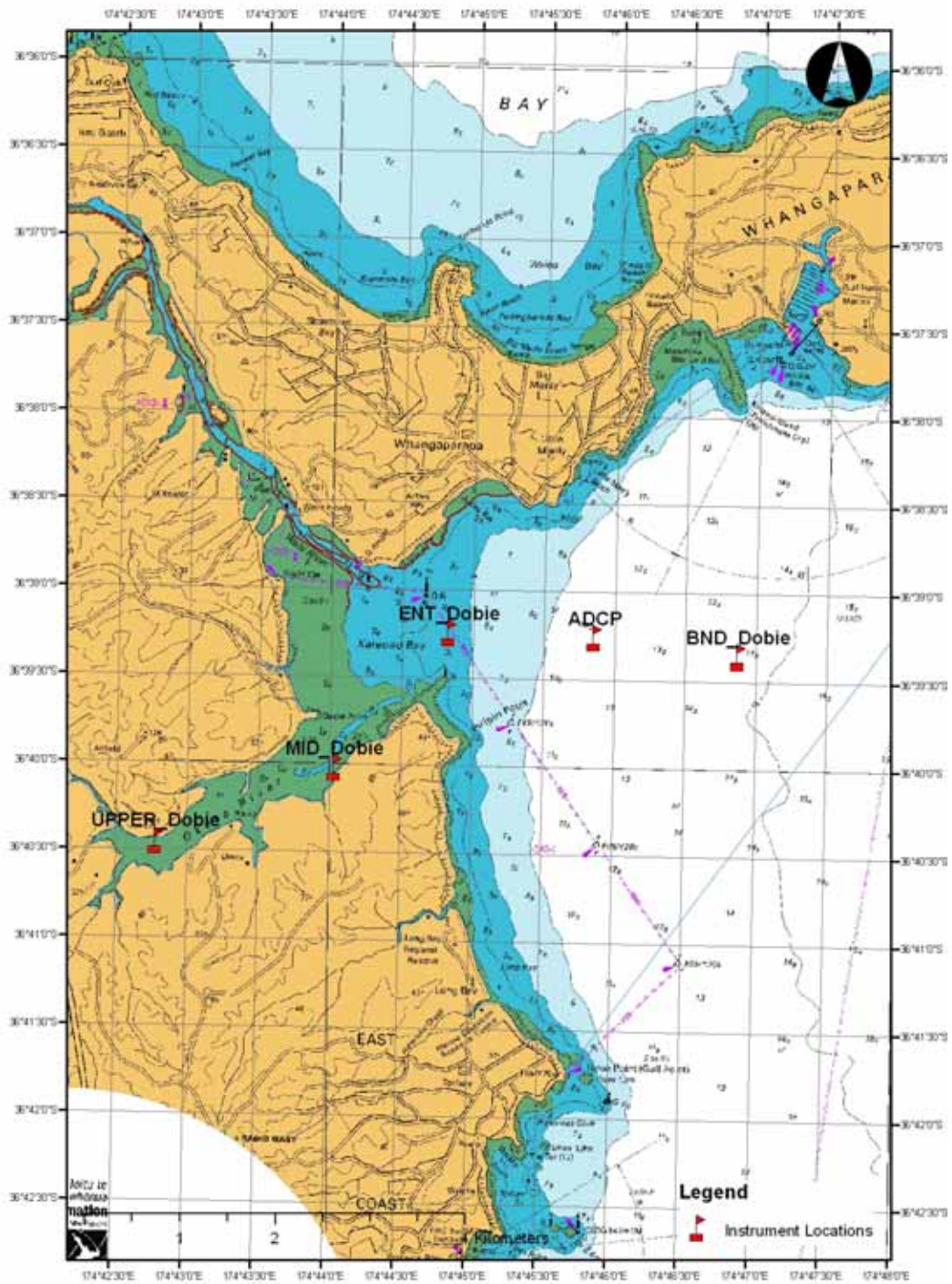
Table 2:

Summary table giving details on mooring name, instrument type, geographical location, dates of deployment and recovery, sample rates and transducer type. OBS = Optical Backscatter Sensor; PT= Pressure Transducer; CT = Conductivity/Temperature

Mooring	Instrument	Location (NZTM)	Date	Δt (s)	Data Type
UPPER	DOBIE	1753076 E 5939909 N		900	OBS, PT, CT
MID	DOBIE	1754963 E 5940668 N	16-10-08	900	OBS, PT, CT
ENT	DOBIE	1756168 E 5942074 N	to	900	OBS, PT, CT
ADCP	ADCP	1757697 E 5942019 N	17-12-08	300	u, v, w, PT
BND	DOBIE	1759208 E 5941819 N		900	PT

Figure 6:

Hydrographic chart (NZ5321) showing the location of the Okura Estuary and instrument mooring deployed between October and December 2008.



2.7 Summary of methodology

The scientific rationale of the study was based on a number of assumptions and conditions:

1. The work and report of Hicks et al. (2009) were used to derive individual catchment event sediment yields (Y) and average freshwater discharge (Q_{avg}).
2. Unmonitored event sediment yields and freshwater discharges from the catchments (OS2-OS9; WE7) surrounding the Okura Estuary (see Figure 1) were scaled relative to the monitored Awanohi catchment (OS4).
3. For MIKE3 FM scenarios, 4 SSC and 4 freshwater point sources were discharged into the MIKE3 FM model domain i.e.:
 - OS2.
 - Catchments OS3 to OS6 are combined as one single source.
 - Catchments OS7 to OS9 are combined as one single source.
 - WE7.
4. MIKE3 FM SSC and freshwater source inputs were discharged into the estuary model over 1 semi-diurnal tidal cycle and then run for a further 7-days
5. Winds were either considered calm or had a constant speed and were held unidirectional for a model simulation i.e., either calm, North-easterly or South-westerly.
6. The model was forced from a single open ocean boundary with only astronomical tidal constituents derived from mooring data.
7. The tidal constituents used to force the open ocean boundary correspond to mean (M_2), Spring (M_2+S_2) and Neap (M_2-S_2) semi-diurnal ranges.
8. The model grid was constructed from chart, survey and LIDAR data. Unresolved subtidal channels in the upper tidal reaches of the Okura estuary were assumed a nominal depth of 0.5 m below chart datum (LAT).
9. 4 specified yields corresponding to 1-month, 3-month, 1-year and 10-year return periods.

The total number of model scenarios = 4 Yields × 3 winds × 3 tidal ranges = 36

Each of the 36 scenarios represents a unique combination of sediment yield, river discharge, windstress and tidal range. The scenarios can be applied by comparing the modelled scenario that most closely matches the observed river discharge, tidal range and speed and direction. The predicted level of sedimentation in response to a scenario maybe then be estimated at each of the selected 'monitored' sites.

3 Model Development, Setup and Calibration

3.1 Modelling overview

Delivery of catchment sediment into the Okura estuary and out into Karepiro Bay is assumed dependent on weather conditions (rainfall/river discharge and wind) and tidal creek dynamics. The model grid or 'mesh' resolution was required to resolve the estuary's main sub-tidal channels from the intertidal areas so that flooding and drying was well represented. This becomes particularly important when considering the re-suspension and transport of intertidal bed sediments.

The MIKE3 FM HD and MT model was run using ocean tides and freshwater/SSC source discharge boundary conditions. The model results were then compared to observations. The model was then calibrated by iteratively changing calibration parameters until modelled and predicted vectors or scalars were in best agreement.

The calibration process determines how well the model can predict tides, currents, suspended-sediment concentrations and salinity at each of the field sites under a range of conditions. Given a good fit between the observed and predicted values the model can be confidently used to make predictions at other sites in the estuary.

3.2 The MIKE3 FM HD and MT model

The Okura estuary was modelled using the DHI MIKE3 FM HD hydrodynamic and MT (mud) sediment transport modelling suite. The finite element, 3-dimensional sigma coordinate (multi-layer) semi-implicit model finds numerical solutions for the Navier-Stokes equations for momentum whilst conserving mass through the principle of continuity. Physical processes in the model can be parameterised / simulated through specifying for example, eddy scales, turbulent closure schemes, surface and bottom boundary conditions, salinity/temperature structure and the earth's rotational effects. The model open boundary is initialised and forced using tidal elevations. Inputs of freshwater are input at source locations, which allow variation in seawater density to be included in model solutions. The finite element grid and baroclinic capability, plus the inclusion of a wetting and drying scheme makes the model ideal for simulating time/spatially varying gravity, density and tidally driven flows in coastal regions with complex shoreline and/or embayments.

The MIKE3 FM HD model can be forced at boundaries by both oceanic/estuarine tides and freshwater sources. These two forcing mechanisms produce the essential boundary physics required to simulate barotropic (tides and surface pressure gradients) and baroclinic (internal pressure gradients driven by horizontal and vertical density differences) in the model domain. The effects of geostrophy, i.e., currents produced by the force balance between pressure gradients and the earth's rotation, are negligible for the size of domain under consideration for this study.

Sediment transport in the MIKE3 FM MT model is simulated through the application of the advection-diffusion (transport) equation. Particles of a specified size may be introduced into the model scheme as a sediment flux associated with each specific freshwater discharge into the model domain. Each specified sediment particle size has a Stokes settling velocity and critical depositional/erosion shear stress. The modelled estuarine hydrodynamics and application of the advection-diffusion scheme then simulate the transport this sediment flux around the model domain. See Appendix 1 for more detail.

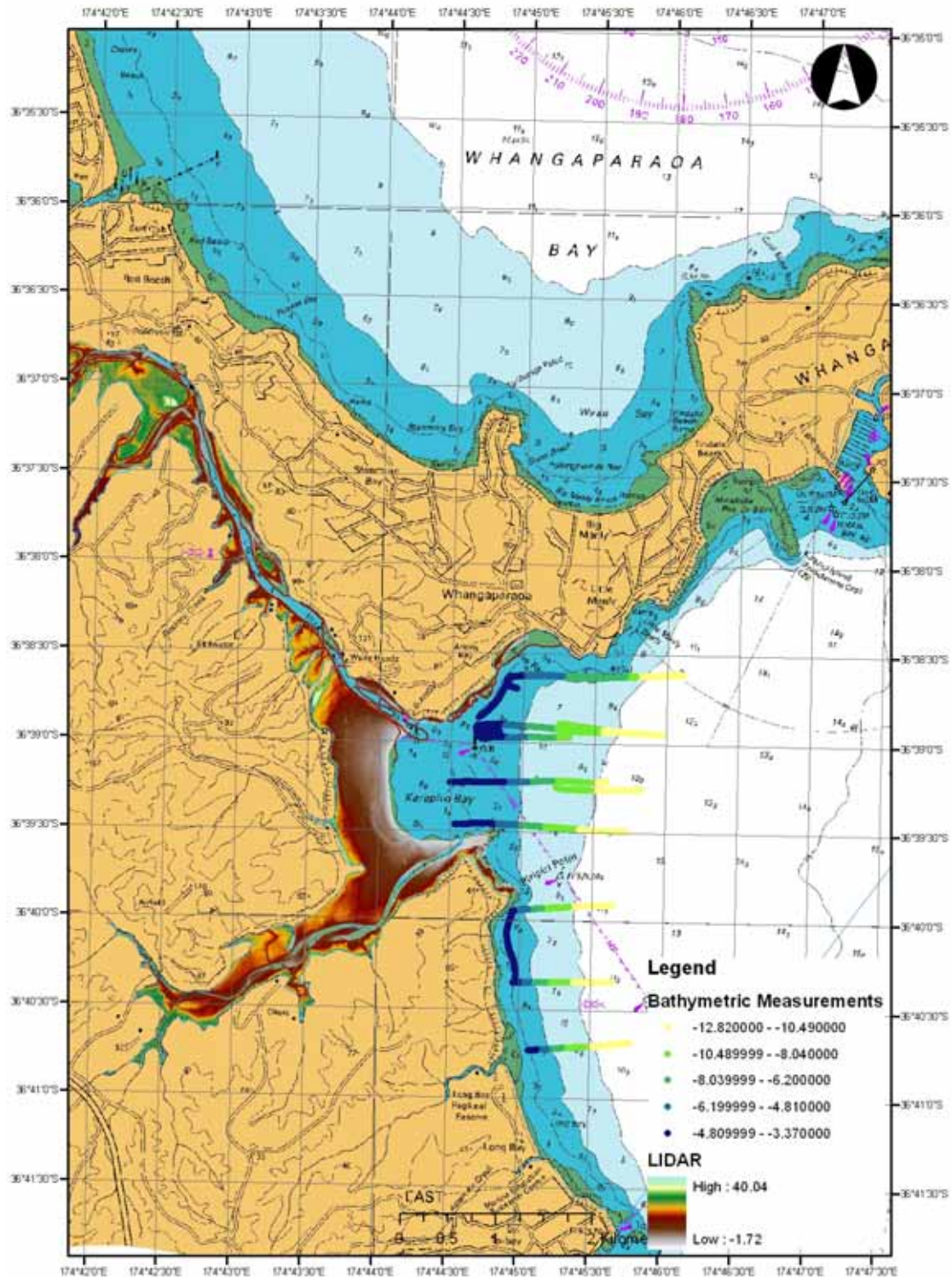
3.3 Model mesh development

The model MIKE3 FM mesh of the Okura estuary and Karepiro Bay was developed through a combination of hydrographic chart data (NZ5321), a bathymetric survey conducted by NIWA on the 21 January 2009 and LIDAR Data provided by the ARC.

The bathymetric survey was completed in 21 January 2009 from the NIWA vessel Rangatahi III using a single point echo-sounder and Trimble RTK DGPS for positioning. The soundings were recorded using HYDROPRO© then tidally corrected and exported to ArcGIS.

Figure 7:

Hydrographic chart (NZ5321) of the Okura Estuary and Karepiro Bay showing areas where LIDAR data and bathymetric surveys were conducted and amalgamated data used to produce the MIKE3 FM model mesh.



High resolution Light Detection and Ranging imagery (LIDAR) data is an aircraft based remote sensing instrument used to collect highly accurate ground levels (relative to local chart datum). The regional coverage of the LIDAR image tiles are shown in Figure 7. Each LIDAR image tile consisted of approximately 1 point per 2 m² with height accuracy mostly ± 0.25 m. These data were then processed into a high resolution raster layer, and a mask of the Okura and Weiti land boundary interface was used to resolve to intertidal areas. The processing of the raw LIDAR data to Chart Datum and into a format readable by the MIKE3 FM models was carried out as outlined in Appendix 2. This data was especially useful for increasing the resolution of the tidal creek and mudflats. However, the channelized region of the estuary that remained flooded at times of low water was not penetrable by the LIDAR instrumentation. Therefore, the channels were assumed to be a nominal depth of 0.5 m below Chart Datum. This did leave some uncertainty on the shape, cross-section and depth in some of the creeks channels. The resultant model mesh produced from all the available data is shown in Figure 8.

Figure 8:

MIKE3 FM HD and MT model mesh produced from a combination of hydrographic charts, LIDAR and bathymetric survey for the Okura Estuary and outflow region into Karepiro Bay. Depth is referenced to lowest astronomical tide (LAT).

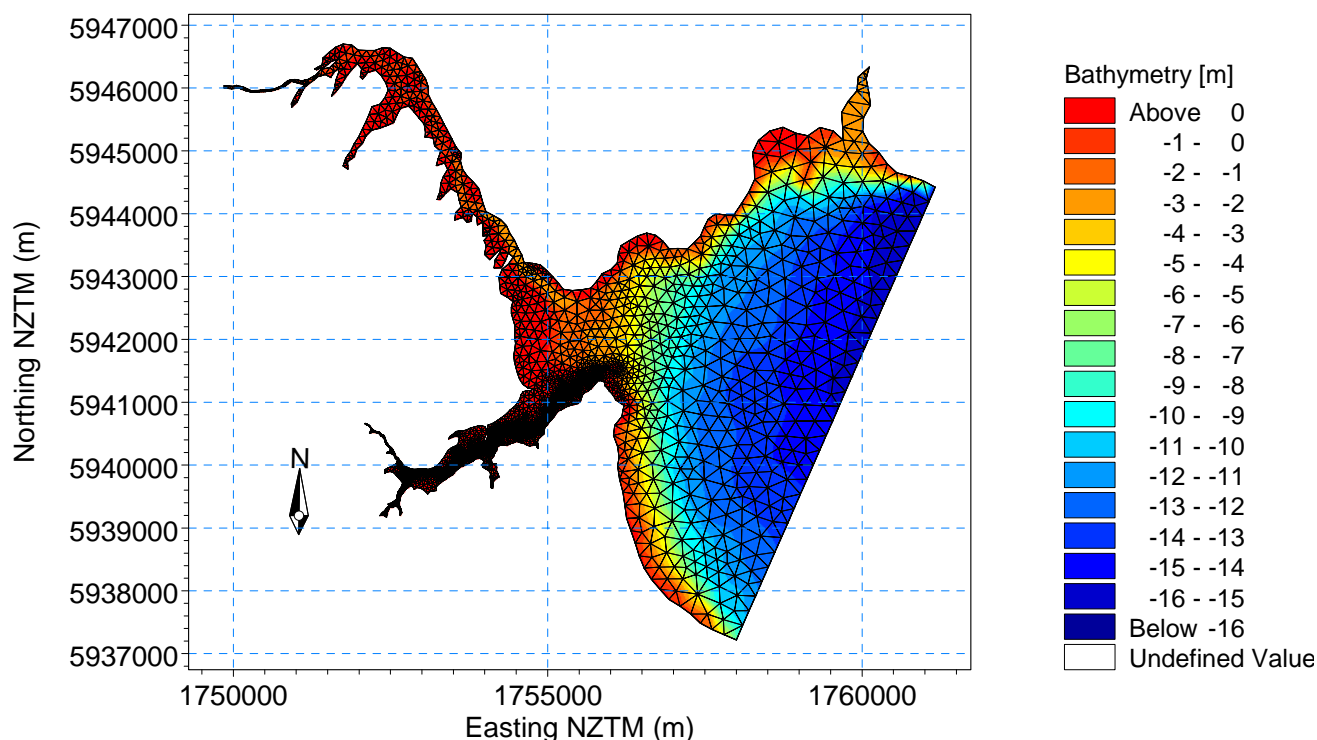


Figure 8 shows the FM mesh generated from all the available bathymetric data. The mesh was produced at a relatively coarse resolution in Karepiro Bay down to finer resolution in the immediate region of the Okura estuary outflow. The estuary mesh resolution was increased further in the estuaries main channel. The mesh element dimensions range with faces having lengths of about 300 m (maximum area 90,000 m²) in Karepiro Bay, and down to approximately 10 m (maximum area 100 m²) in the main estuary channel.

3.4 Calibration parameters

The MIKE3 FM HD model was calibrated by achieving a 'best fit' between the model and coincident observations. Parameters that were 'adjusted' in the model to achieve a best fit between modelled and observed values were the:

- Smagorinsky eddy coefficient: Simulates horizontal shear in the model and causes change in the amplitude of surface elevations and the magnitude of current speeds.
- k - ϵ Vertical turbulence closure: Controls mixing in the vertical and impacts on vertical stratification in the model due to freshwater inputs.
- Bed roughness (z_0): Controls the phase (timing) of sinusoidal signals as for example, tidal elevations and currents.

The measure of the 'goodness of fit' between observed and predicted was then estimated through the:

- Root mean square error (RMSE) – A measure of the difference in the variance between the observed and predicted signal.
- Cross-correlation – A coefficient that describes the strength in the phase relationship (timing) between two oscillating signals. 0-1, with 0 being weak and 1 being strong
- Bias: The residual offset between two time series. \pm bias indicates a positive/negative offset in time series data.

3.5 Calibration data

The process of model calibration consists of running a model simulation with the correct boundary conditions for the period when field data were collected and then comparing the observed field data with the model predictions. Model parameters are then adjusted until the best fit between the observations and predictions is obtained.

Tidal elevation, conductivity and temperature (salinity) and current meter data recorded by DOBIES and the ADCP current meter were used to calibrate the MIKE3 FM HD model. Optical Backscatter (OBS) data recorded by the DOBIEs was used to calibrate

the MIKE3 FM MT sediment transport model as discussed in later sections. All mooring and instrument details for the calibration are presented in Table 2.

3.6 Offshore tidal boundary conditions

The Okura MIKE3 FM HD model was forced at the ocean boundary by tidal elevation data recorded by the DOBIE at Site BND (see Figure 6). This time-series of pressure data covered the best part of the 2-month deployment period. After instrument recovery the pressure data was converted to depth assuming the hydrostatic approximation. The mean depth of the time-series was then subtracted leaving the sea surface elevations used to force the model.

The Okura model open ocean boundary as shown in Figure 8 extended some 8 km from Toroa Point to Rakauananga Point. To account for the phase lag of the Kelvin wave across the boundary, a graduated 1-minute sea surface elevation across the North-South open boundary was implemented and used as the model boundary condition.

3.7 Wind forcing

The wind induced shear stress (τ_w) was computed from local wind speed and direction measurements made at Whangaparaoa Airport and included in model calibration runs.

3.8 Calibration of water surface elevations

Figure 9 to Figure 11 shows comparisons between the observed and modelled sea surface elevations at the mooring site locations shown in Figure 6 and listed in Table 2. The results of the RMSE, cross correlation and bias analysis are also shown in Table 3.

Results from the error analysis between the observed and modelled sea surface elevations showed a 7 to 15 cm error in RSME and 0 to 3 cm in the bias. The model predictions tended to over predict low water levels i.e., model values indicated a lower water level than that observed, especially at low water spring tides. This was a result of siting the DOBIE instruments in deeper holes in the estuary channels for protection and to try and avoid exposure of the moorings at low water spring tides. However, as a consequence this did lead to the deviations in the modelled and observed sea surface elevations. Cross-correlation coefficients were better than 0.99 indicated excellent phase agreement between the observed and modelled elevations.

Aside from some deviations at low water, the model generally represented water levels well, indicating that the volume and timing of tidal exchange between Okura Estuary and Karepiro Bay was correct.

Figure 9:

Observed and modelled sea surface elevation for the UPPER DOBIE mooring site (see Figure 6) for the period 16 October to 17 December 2008. Time axis is shown in year day format.

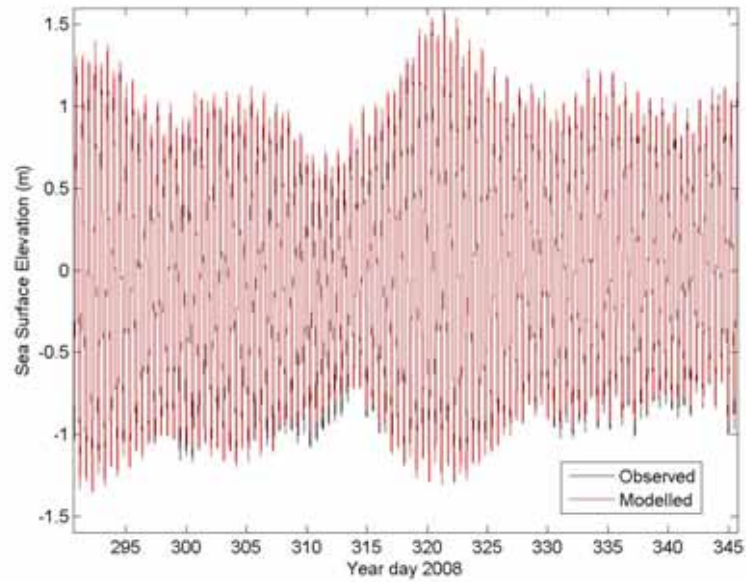


Figure 10:

Observed and modelled sea surface elevation for the MID DOBIE mooring site (see Figure 6) for the period 16 October to 17 December 2008. Time axis is shown in year day format.

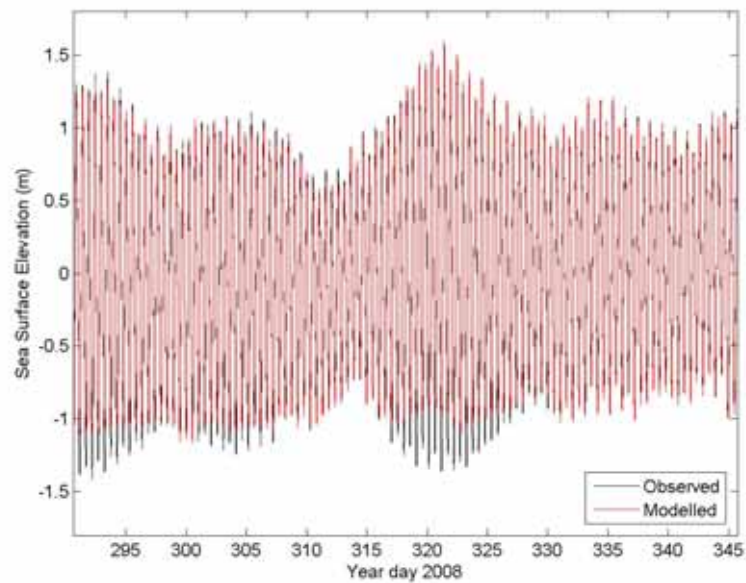


Figure 11:

Observed and modelled sea surface elevation for the ENT DOBIE mooring site (see Figure 6) for the period 16 October to 17 December 2008. Time axis is shown in year day format.

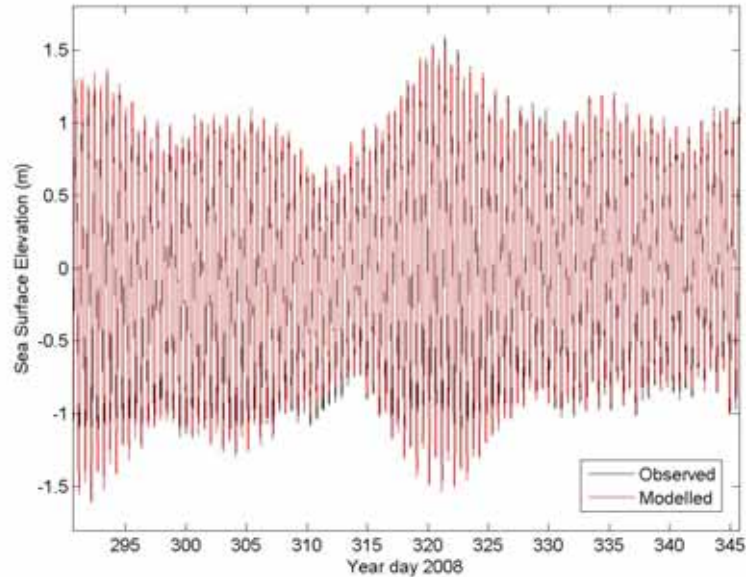


Table 3:

Summary error statistics between observed and modelled sea surface elevation at the 3 DOBIE sites (see Figure 6) in the Okura estuary for the period 16 October to 17 December 2008 spanning the mooring deployments.

Site	RMSE (m)	Cross-Correlation	Bias (m)
UPPER	0.07	0.99	-0.03
MID	0.1	0.99	-0.01
ENT	0.15	0.98	0

3.9 Calibration of currents

The calibration of model flow velocities was limited to a comparison with data from a single ADCP current meter moored at a site in Karepiro Bay as shown in Figure 6. Figure 12a and Figure 12b show the resultant from the direct comparison between time series of observed and modelled depth-averaged u (East-West) and v (North-South) components of velocity.

Figure 12a:

Observed and modelled depth averaged current velocities as recorded at the ADCP mooring site between the dates 16 October to 12 November 2008. Time axis is shown in year day format.

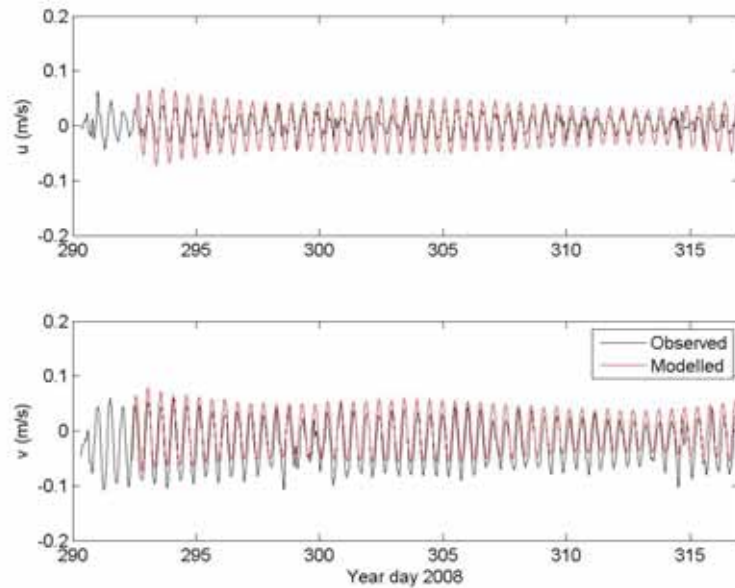
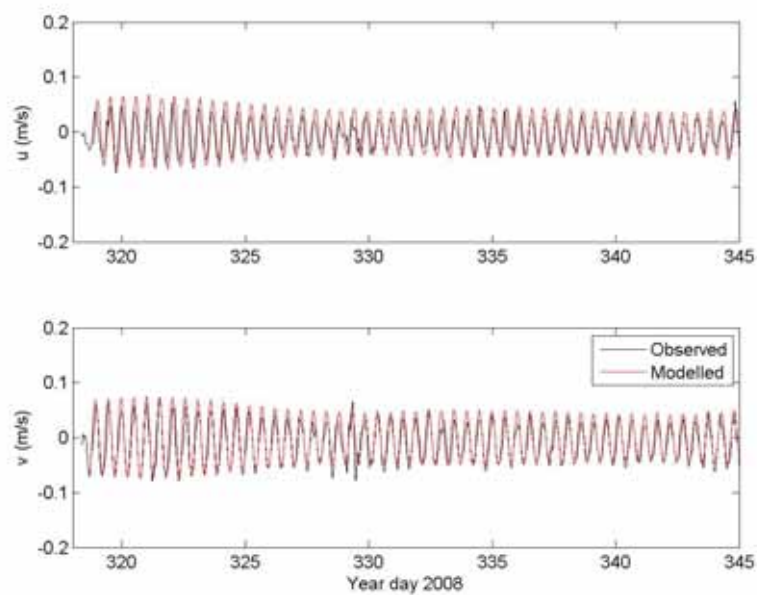


Figure 12b:

Observed and modelled depth averaged current velocities as recorded at ADCP mooring site between the dates 12 November to 17 December 2008. Time axis is shown in year day format.



The best overall fit between observed and model predictions was obtained by using a Smagorinsky horizontal eddy viscosity coefficient of 0.28 for the horizontal eddy viscosity formulation, with a lower bound of $1.8 \times 10^{-6} \text{m}^2/\text{s}$ and an upper bound of $10 \text{m}^2/\text{s}$. The vertical turbulence closure in the MIKE3 FM model is based on a standard $k-\varepsilon$ model, with a buoyancy extension (e.g., Rodi, 1980, 1984). This closure model uses transport equations for the turbulent kinetic energy (TKE), k , and the dissipation of TKE, ε , to describe the turbulence. Details of all the constants and coefficients used in the turbulence module are shown Table A1.

Table 4:

Summary error statistics between the observed depth averaged current meter records and model predictions for both of the 2008 ADCP deployment periods.

Deployment 1	RMSE (m/s)	Cross-Correlation	Bias (m/s)
u	0.02	0.76	0
v	0.07	0.87	-0.02
Deployment 2			
u	0.02	0.72	-0.01
v	0.06	0.84	-0.01

Visual comparisons of the observed time series with the modelled currents indicated reasonable agreement as supported by the error analysis shown in Table 4. The bias for both current meter deployments was exceptionally small i.e., $O(1 \text{ cm})$ and within error bounds of the ADCP data. The cross-correlation analysis suggested reasonably good agreement in phasing between the observed and modelled currents although visually, the predictions for the second deployment appeared in better agreement. This may be regarded as a good calibration for an open-embayment site and it demonstrates that the tidal forcing at the boundary is adequate to describe most of the flow in Karepiro Bay. Adjusting the wind drag coefficient (C_d) for the wind induced shear stress computed from the local Whangaparaoa weather records made no significant improvements to the calibration.

Tables 5a-5b show the results from a least squares tidal harmonic analysis (Pawlowicz et al. 2002) of both modelled and observed current phase and amplitude for both of the ADCP deployment periods. Current amplitude was defined in terms of the ellipse major amplitude (maximum tidal current along the principal axis of the current) and ellipse inclination (peak tidal current direction relative to True North), and ellipse phase (time of the peak tidal current relative to NZST). Only tidal constituents with signal to noise ratios (SNR) > 2 are reported (there are many other tidal constituents that could not be resolved because the record durations were too short).

The principle lunar (M_2) and principle solar (S_2), the dominant tidal components around the New Zealand coast were adequately resolved at the ADCP site by the tidal analysis. The observed and modelled amplitudes for both the M_2 and S_2 constituent were in good agreement. However, the ellipse inclination phase differences between the observed and modelled tidal ellipses did show discrepancies of up to 40 deg. The reasons for these differences are due to discrepancy in phase lags across the forced boundary. Without an array of current meters this cannot be accurately resolved. However, this has little consequence at the sites of interest for this study.

Table 5a:

Comparison of measured and predicted depth averaged tidal current ellipses at the ADCP mooring site for the period 16 October to 12 November 2008.

Location	Observed			Modelled			Difference		
	Amplitude (m/s)	Inclination (° True)	Phase (° NZST)	Amplitude (m/s)	Inclination (° True)	Phase (° NZST)	Amplitude (m/s)	Inclination (°)	Phase (°)
M2 Principle Lunar	0.06	72	312	0.06	51	272	0	21	40
S2 Principle Solar	0.01	87	17	0.01	46	33	0	41	16

Table 5b:

Comparison of measured and predicted predicted depth averaged tidal current ellipses at the ADCP mooring site for the period 12 November to 17 December 2008.

Location	Observed			Modelled			Difference		
	Amplitude (m/s)	Inclination (° True)	Phase (° NZST)	Amplitude (m/s)	Inclination (° True)	Phase (° NZST)	Amplitude (m/s)	Inclination (°)	Phase (°)
M2 Principle Lunar	0.06	55	308	0.06	52	286	0	3	22
S2 Principle Solar	0.01	36	25	0.01	51	2	0	34	23

3.10 Salinity

The MIKE3 FM HD was calibrated at 3-estuary sites: two sites located inside the estuary in sub-tidal channels at the UPPER and MID sites; one site located in the estuary entrance at Site ENT (see Figure 6).

The DOBIE instruments measured salinity only at one fixed depth, approximately 0.75 metres above bed. Therefore, these measurements did not give any detail on stratification through the water column. Nevertheless, during the flood and early phases of the ebb tide, we assume tidal straining has mixed the water column. Therefore, we can assume the DOBIEs then give a good measure of the salinity in a homogenous water column. In addition, good agreement between the observed and modelled salinity would indicate that freshwater discharge used as a model boundary condition into the estuary was also in the correct order.

Figure 13a and Figure 13b show a comparison between the observed and modelled salinities for the 3 instrumented DOBIE sites during two separate periods inclusive of the instrument deployments.

At the UPPER site, the comparisons shown Figure 13a and Figure 13b illustrates a good phase relationship between the observed and modelled salinities. The modelled

salinities at the UPPER site oscillated in a range of approximately 26 to 30 PSU at semi-diurnal tidal frequencies.

Further downstream at the MID site both the observed and modelled salinities shown in Figures 13b illustrate only small oscillatory changes of order 1-3 PSU. At the estuary's entrance, both the observed and modelled salinities at the ENT site showed little deviation from regional open water salinity values of 33.5 PSU.

The model tended to slightly under predict the range of salinity variation as observed in the upper estuary. This results from a combination of discrepancies in the model grid (volume), error in the estimated river discharge and the vertical turbulence closure scheme ($k-\epsilon$) slightly under predicting the intensity of vertical mixing.

The modelled salinities at the two DOBIE sites downstream and in the estuary entrance were in better agreement with the observations. However, due to the depth of water at these two sites, the DOBIES did not provide any detail of near surface stratification during the ebb phase of the tide.

Figure 13a:

Observed and modelled salinities for the period extending from 12 October to 1 December 2008 at Sites (a) UPPER; (b) MID and (c) ENT in the Okura estuary. Time axis is shown in year day format.

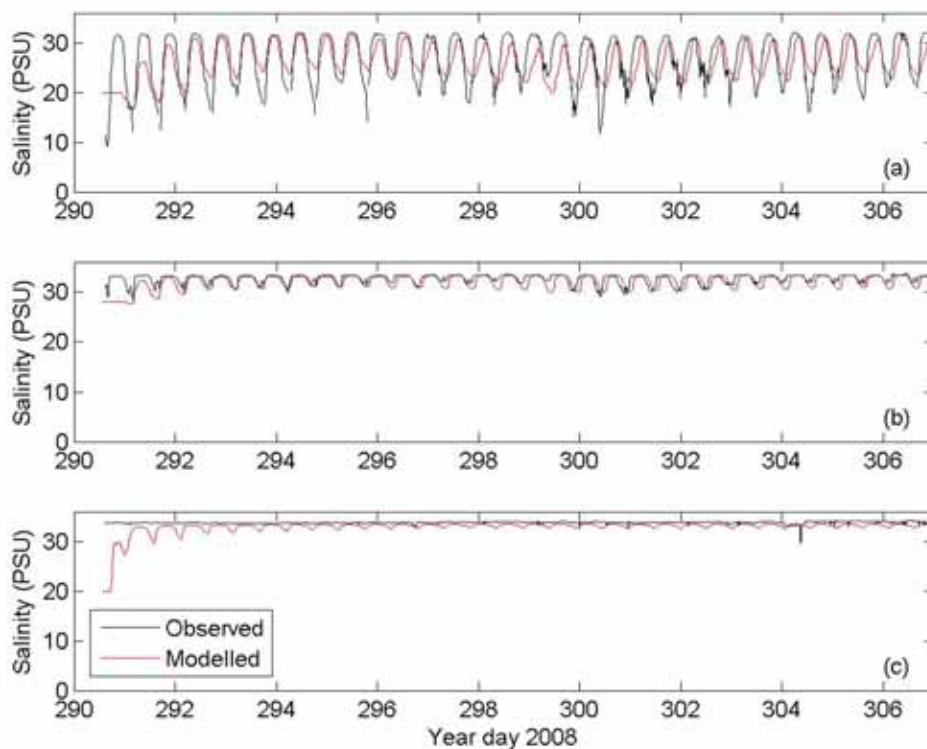


Figure 13b:

Observed and modelled salinities for the period extending from 11 November to 29 November 2008 at Sites (a) UPPER; (b) MID and (c) ENT in the Okura estuary. Time axis is shown in year day format.

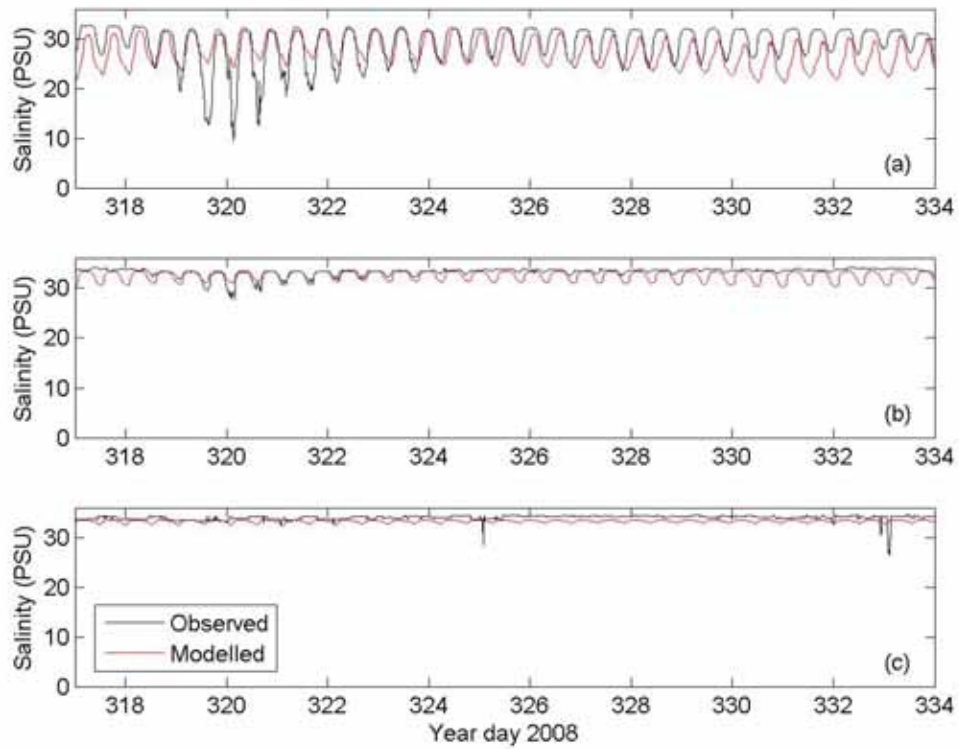


Table 6:

Summary error statistics between the observed and modelled salinities at the 3 DOBIE mooring sites for the two salinity calibration periods.

Deployment 1	RMSE (PSU)	Cross-Correlation	Bias (PSU)
UPPER	4.62	0.40	0.86
MID	1.51	0.31	0.56
ENT	1.78	0.09	0.92
Deployment 2			
UPPER	4.51	0.24	1.74
MID	1.41	0.19	0.78
ENT	0.94	0.10	0.75

3.11 MT sediment transport module calibration

The MIKE3 FM MT sediment transport model as described in Appendix 1 requires information about sediment particle size and fall velocity; critical thresholds for deposition and erosion of the particles. A study by Green and Coco (2007) indicates that sediment coarser than fine sand is not likely to be mobilised in any significant way by waves and currents in enclosed coastal regions. Hence, any sediment coarser than fine sand is considered here to be “relict”, and does not contribute to the suspended-sediment load in the model. This is not to say that coarser sediment will never be moved; wave and current conditions will at times cause the re-suspension and transport of sand-sized material even in relatively sheltered coastal areas, while sand transport will be a regular occurrence in exposed areas with fast tidal currents, such as near to an estuary inlet throat. However, finer sediment transport in relatively sheltered areas is the focus of this study. Therefore, a particle grain size of 15 μm was used in the sediment transport model, corresponding to a fine to medium silt sediment fraction.

3.12 Observations and MT module setup

Figure 14 shows the results from both the observed and modelled SSC for the UPPER and MID DOBIE sites in the Okura estuary. The DOBIE OBS moored at the ENT side failed due to excessive bio-fouling. The observed time series shows a background SSC of approximately 0.05 kg/m³ with SSC increasing during spring tidal ranges (see Figure 14c) in response to increased bed shear stresses. The gaps in the observations are due to exposure of the OBS at low water and the isolated peaks that appear randomly in the SSC time are generated by local wind wave re-suspension, which was not included in the model.

The MT model was initially set up using a sediment grainsize of 15 μm . By assuming a sediment density of 2650 kg/m³ (quartz), the Stokes fall velocity was set at 0.0002 m/s. The bed density in the model domain was fixed at 1200 kg/m³ (McDowell and O'Connor, 1977). The critical bed shear stress for erosion τ_{ce} was set for cohesive type sediments at 0.15 N/m² for freshly deposited sediments (Whitehouse et al. 2000). Therefore, the τ_{ce} for the whole of the model domain was set to 0.15 N/m². The critical bed shear stress for deposition was set at $\tau_{cd} = \tau_{ce}/2$ (Whitehouse et al. 2000). Sediment source concentrations were set at a constant 0.05 kg/m³, corresponding to the baseline concentrations measured by the DOBIE instrumentation.

Bed erosion rate (E) in the MT module was modelled through a soft bed parameterization (see Appendix 1) to simulate mainly freshly deposited sediment (Parchure and Mehta, 1985). The erosion coefficient α and an excess bed shear stress ($\tau_b - \tau_{ce}$) evolve the erosion rate exponentially and are ultimately based on the modelled current speeds and drag at the bed. Thus sediment transport depends on current speed multiplied by a high power. This becomes especially important during spring tides as the bed shear stress increases due to an increase in the magnitude of

tidal currents, and so considerably more sediment transport occurs during spring tides than at neaps.

Figure 14:

Time series of observed and modelled SSC for (a) UPPER DOBIE site; (b) MID DOBIE SSC and (c) observed sea surface elevations at the MID DOBIE for the time period 5 November to 25 November 2008. Time axis is shown in year day format.

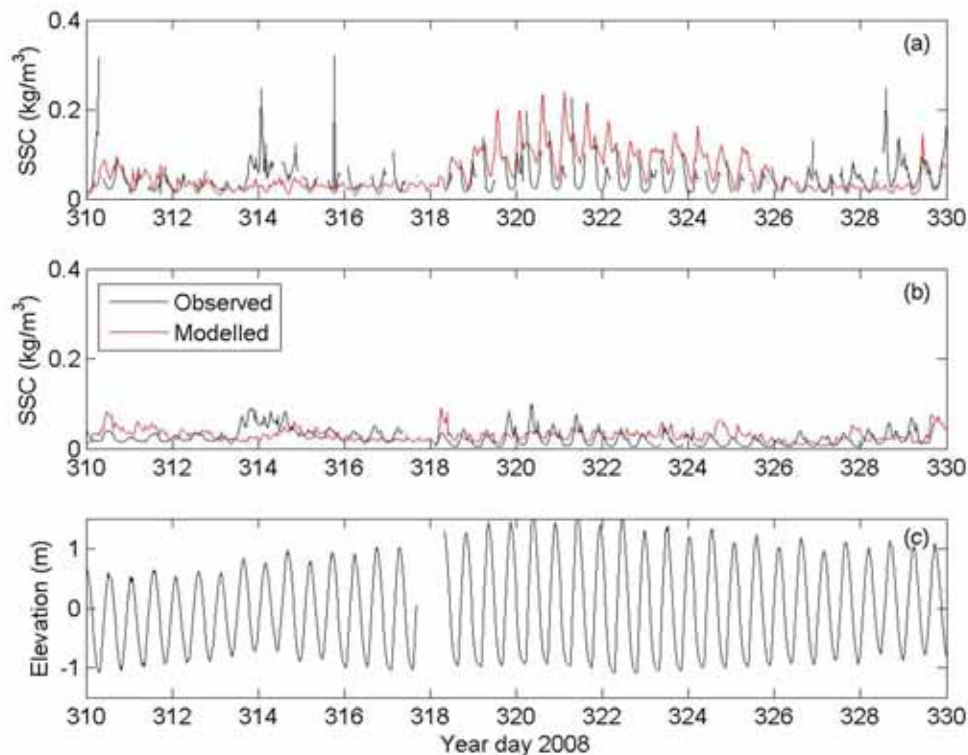


Figure 15 illustrates an example of published erosion rates (Van Rijn, 1989; Houwing, 1999; Whitehouse, 2000; Andersen and Pejrup, 2001; Wang, 2003) for similar physical settings and grainsize used in this study. The α and E_c values were set at $E_c = 0.00005 \text{ kgm}^{-2}\text{s}^{-1}$ and $\alpha = 4.3$ in our model. These values were set to reflect the higher side of published values. A potentially higher incidence of sediment re-suspension and remobilisation in the model due to higher rates of erosion at higher values of excess bed shear stress would produce a cautionary (slightly high) result for transport and deposition of sediments at the sites of specific interest.

Figure 15:

Comparison of 5 published erosion rates and the erosion rate (Mike MT) used in the MIKE3 FM MT model setup for the Okura estuary.

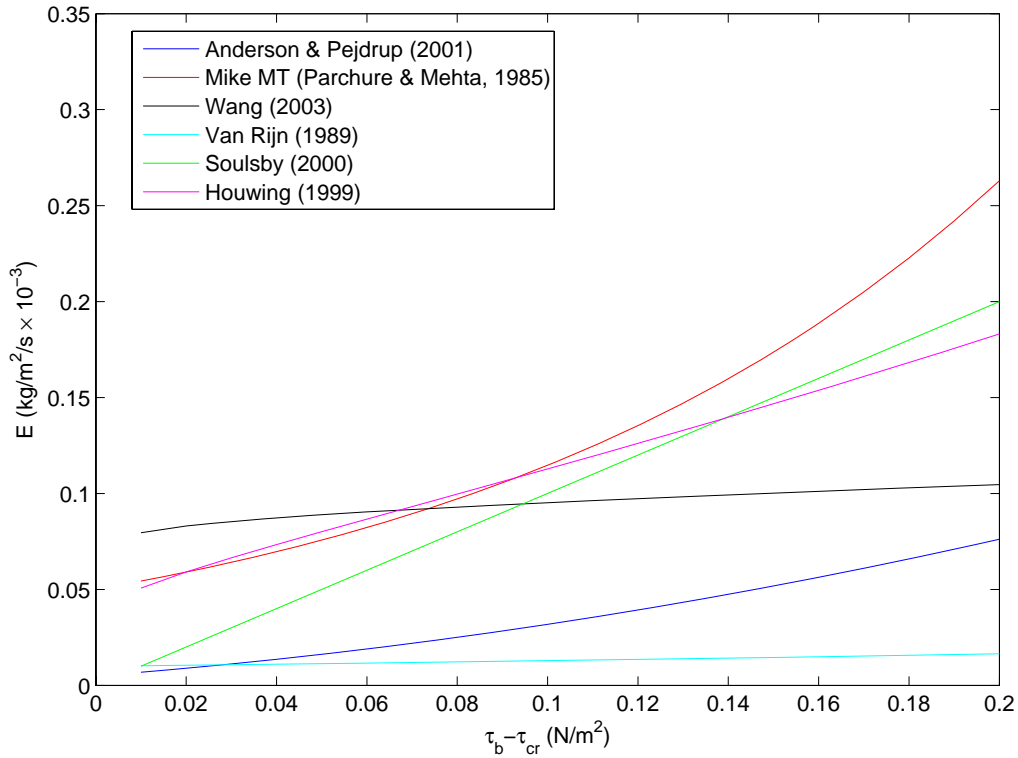


Figure 14 illustrates the model results as compared to the observed levels of SSC. This was a result of first spinning the model up for 10-days prior to the period selected for the calibration. The initial calibration runs indicated too much sediment was remaining in suspension. Therefore, the critical bed shear stress for erosion and deposition was increased to 0.2 N/m² and 0.1 N/m² respectively to achieve the better result. The model thereafter simulated the observed oscillations in SSC during tidal excursions and during spring tides (i.e., Figure 16). However, the model did not produce the odd random peaks in observed SSC because orbital velocities from surface wave re-suspension and mobilisation were not included in the model. Figure 16 shows a plot of observed SSC versus modelled for both the UPPER and MID DOBIE sites. The comparison illustrates considerable scatter at higher SSC. A summary of comparative error statistics for the observed and modelled SSC data are shown in Table 7. Cross-correlation analysis was not performed on these data sets due to gaps in time series data due to DOBIE OBS dropout. Bias estimates were small but RMSE errors were large and reflected the high variances in the time series caused by the wind wave re-suspension that was not simulated in the model.

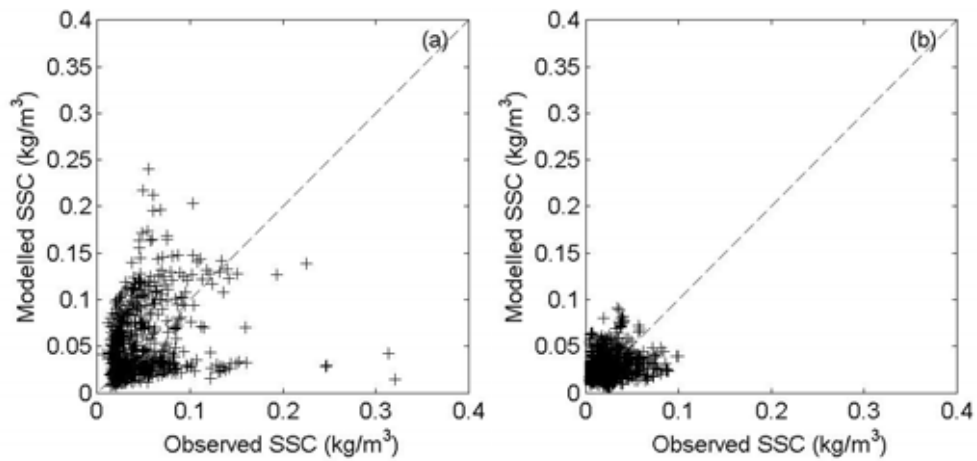
Table 7:

Summary error statistics between the observed and modelled SSC at the 2 DOBIE mooring sites for the time period 5 November to 25 November 2008.

Mooring	RMSE (kg/m^3)	Bias (kg/m^3)
UPPER	0.05	-0.01
MID	0.02	0

Figure 16:

Observed SSC versus modelled SSC for (a) UPPER and (b) MID DOBIE mooring sites for the time period 5 November to 25 November 2008. Stippled line represents 1:1 ratio of observed and modelled SSC.



4 MT Model Scenario Setup

The MT model was setup to provide a series of look up tables that contain suspended sediment mass and bed deposition mass for a series of event driven catchment discharge scenarios. Each value in a table was derived from a specific model scenario. Each model scenario is based on combinations of:

1. A specific tide i.e., 7-day spring range; 7-day neap range and 7-day average range tides. Each scenario was initialised with a 'hotstart' or spun up hydrodynamic model field for each tidal range scenario for model stability.
2. Specific wind events i.e., calm, 7.5 m/s North-easterly and South-westerly as described in Section 2.
3. A series of specific freshwater and sediment discharge rates from identified sources based on return periods of specific yield from monitored catchments and rivers in the region of the Okura.

Further details of scenario setup and experimental rationale were presented in Section 2. Results from the application of the model to the ecological monitoring in the Okura Estuary and Karepiro Bay are presented in a separate report.

5 Summary

Observed and modelled sediment yield data and river discharge rates from several freshwater sources inputs into the Okura estuary were used to arrive at 4-return period storm runoff scenarios. Each scenario provided a suspended sediment load and river discharge that could be incorporated as a numerical model source input. Further analysis of local meteorological data provided bi-directional (North-east/South-west) wind data for the region that also would be used to force later model scenarios.

A MIKE3D FM hydrodynamic model (HD) mesh of the Okura Estuary and Karepiro Bay was constructed from local hydrographic charts, a small bathymetric survey and LIDAR data. The model was forced with freshwater source inputs and tides which were measured at the open boundary. Further observations of depth, salinity and a single current meter were used to calibrate the model.

Simulated surface elevations compared well with those observed at mooring sites. Bias, and RMSE were $O(0.1\text{m})$ and correlation coefficients were $O(0.99)$. Comparisons of modelled data with a single current meter site measurement showed reasonable agreement. The bias $O(0.2\text{ cm/s})$ and RMSE $O(0.4\text{ cm/s})$ were small as compared to the overriding signal. A comparison of the tidal analysis of the observed and predicted currents indicated reasonable agreement in the amplitude, inclination and phase of the dominant (M_2 , S_2) tidal ellipses.

The salinity calibration of the model proved more testing as measurements taken near the sea bed by the DOBIE moorings did not divulge any information on water column stratification. However, the predictions at all 3-DOBIE sites reproduced the tidally modulated salinity oscillations although the phasing between the observed and modelled was slightly out. This was thought to be due to subtle difference in the estimated and actual bathymetry causing non-linear shifts in tidal phase of the observed salinity not simulated by the model. Both bias and RMSE estimated were small.

The MIKE3D FM mud transport module (MT) was used to model the sediment discharged from the sources into the estuary. A nominal $15\text{ }\mu\text{m}$ particle was used in simulations. The modelled SSC at 2-DOBIE sites after initial changes in the threshold calibration parameters produced similar trends as the observations. Comparisons of the observed and modelled data was difficult because the DOBIE's OBS's became exposed at tidal low water level. Thus no record was available for a continuous model-observed data analysis. Nevertheless, bias estimates were small. RMSE values which were quite large as compared to the signal were a result of large peaks in the data series generated by wind wave resuspension not simulated by the model.

The calibration was deemed satisfactory and ready for implementation and use for the 36 event driven scenario runs to produce lookup tables.

6 Acknowledgements

The authors would like to thank Megan Stewart, and Grant Barnes from Auckland Regional Council; Nicole Hancock, Cliff Hart, Rod Budd, Scott Stephens, Luca Chiaroni and Aslan Wright-Stow for fieldwork and Murray Hicks for the sediment yield data.

7 References

- Andersen, T.J.; Pejrup, M. (2001). Suspended sediment transport on a temperate, microtidal mudflat, the Danish Wadden Sea. *Marine Geology* 173: pp. 69-85.
- Fofonoff, P. & Millard, R.C. Jr. (1983). Algorithms for computation of fundamental properties of seawater, 1983. _Unesco Tech. Pap. in *Mar. Sci., No. 44*, 53 pp.
- Fredsoe, J. (1984). Turbulent boundary layer in wave-current motion. *Journal of Hydrological Engineering, A.S.C.E, Volume 110*, HY8, 1103-1120 (1984).
- Green, M.O.; Coco, G. (2007). Sediment transport on an estuarine intertidal flat: measurements and conceptual model of waves, rainfall and exchanges with a tidal creek. *Estuarine, Coastal and Shelf Science* 72: 553-569.
- Hicks, D.M.; Hoyle, J.; Roulston, H. (2009). Analysis of Sediment Yields Within Auckland Region. Prepared by NIWA for Auckland Regional Council. Auckland Regional Document Type 2009/#####.
- Houwing, E.J. (1999). Determination of the critical erosion threshold of cohesive sediments on intertidal mudflats along the Dutch Wadden Sea Coast. *Estuarine, Coastal and Shelf Science* 49: pp. 545–555.
- McDowell, D.M.; O'Connor, B.A. (1997). Hydraulic Behaviour of Estuaries. Macmillan Press Ltd, London, UK. ISBN 0 333 12231 3.
- Parchure, T.M. & Mehta, A.J. (1985). Erosion of soft cohesive sediment deposits. *Journal of Hydraulic Engineering* 111: 1308–1326.
- Pawlowicz, R.; Beardsley, B. & Lentz, S. (2002). Classical tidal harmonic analysis including error estimates in MATLAB using T_TIDE". *Computers and Geosciences* 28: 929-937.
- Rodi, W. (1980). Turbulence models and their applications in hydraulics-A state of the art review, Special IAHR Publication.
- Rodi, W. (1984). Turbulence models and their applications in hydraulics, IAHR, Delft, the Netherlands.

- Swales, A.; Hume, T.M.; McGlore, M.S.; Pilvio, R.; Ovenden, R.; Zviguina, N.; Hatton, S.; Nicolls, P.; Budd, R.; Hewett, J.; Piickmere, S.; Costely, K. (2002). Evidence for the physical effects of catchment sediment runoff preserved in estuarine sediments: Phase II (field study). ARC Technical Publication 221 NIWA Client Report HAM2002-067.
- Soulsby, R.L.; Hamm, L.; Klopman, G.; Myrhaug, D.; Simons, R.R.; Thomas, G.P. (2000). Wave-current interaction within and outside the bottom boundary layer *Coastal Engineering 21*: 41-69.
- van Rijn, L.C. (1989). Handbook on Sediment Transport by Current and Waves. *Delft Hydraulics*, Report H461, pp. 12.1-12.27.
- Wang, Y.H. (2003). The intertidal erosion rate of cohesive sediment: a case study from Long Island Sound. *Estuarine, Coastal and Shelf Science 56*. pp. 891–896.
- Whitehouse, R.; Soulsby, R.; Roberts, W.; Mitchener, H. (2000). Dynamics of estuarine muds. Thomas Telford.

8 Appendix 1: Formulation of processes simulated by the MIKE3 models

This section outlines the methods used by the MIKE3 FM HD and MT models to simulate tidal propagation within the harbour, tide- and wind-driven currents, freshwater mixing and sediment transport.

8.1 Bed shear stress

MIKE3 FM HD uses a quadratic friction law to define the bed shear stress due to the current:

$$\frac{\bar{\tau}_b}{\rho_0} = c_f \bar{u}_b |\bar{u}_b|$$

where c_f is the drag coefficient, \bar{u}_b is the time-averaged current speed at a distance Δz_b above the bed, and ρ_0 is the density of water. The drag coefficient is defined in terms of a logarithmic profile between the seabed and the point Δz_b above the seabed:

$$c_f = 1 \frac{1}{\left(\frac{1}{\kappa} \ln \left(\frac{\Delta z_b}{z_0} \right) \right)^2}$$

where $\kappa = 0.4$ is von Karman's constant and z_0 is the bed roughness length, which is typically varied to calibrate the model.

where k is the bed roughness and a is the wave-orbital semi-excursion at the bed. Also, f_c is the pure-current friction factor, given by the logarithmic resistance law:

8.2 Currents

The influence of the wind on currents is treated in terms of the wind-induced shear stress that acts on the sea surface:

$$\tau_w = \rho_a c_d |u_w| u_w$$

where ρ_a is the density of air, c_d is the drag coefficient and u_w is the wind speed 10 m above the sea surface. The model is typically calibrated by adjusting c_d .

The turbulent transfer of momentum by eddies gives rise to an internal fluid friction which is resolved in the horizontal and vertical dimensions by use of an eddy viscosity formulation.

In the vertical, the eddy viscosity is derived from k - ε formulation where eddy viscosity is determined from the k or production term and ε the dissipation term (Rodi, 1980, 1984). The turbulence module is parameterised through a series of empirical coefficients.

For the horizontal eddy viscosity, the Smagorinsky formulation was applied, which gives the sub grid-scale eddy viscosity as:

$$A = c_s^2 l^2 \sqrt{2S_{ij}S_{ij}}$$

where c_s is a constant, l is the characteristic length (approximated by the minimum edge length for each element) and the deformation rate (S_{ij}) is given by

$$S_{ij} = \frac{1}{2} \left(\frac{\partial u_i}{\partial x_j} + \frac{\partial u_j}{\partial x_i} \right)$$

Using this formulation, the model can be calibrated by adjusting the constant c_s and by defining the upper and lower limits of the horizontal eddy viscosity.

8.3 Salinity

In baroclinic mode MIKE3 FM HD requires coefficients for vertical and horizontal dispersion. These can be constant or they can be proportionally scaled to the eddy viscosity. For the implementation of the model here a scaled dispersion coefficient was used.

8.4 Sediment transport

MIKE3 FM MT can simulate the erosion, transport and deposition of up to 8 different grainsize fractions. For each grainsize a fall velocity (w_s) is assigned.

8.4.1 Deposition

Deposition of sediment onto the bed is deemed to occur when and where the bed shear stress (τ_b) is smaller than the critical bed shear stress for deposition (τ_{cd}). A separate τ_{cd} is assigned to each grainsize.

The deposition rate ($\text{kg}\cdot\text{m}^{-2}\cdot\text{s}^{-1}$) is given separately for each grainsize by:

$$D = w_s \rho_d c_b$$

where ρ_d is the probability ramp function for deposition defined as:

$$p_d = \max(0, \min(1, 1 - \frac{\tau_b}{\tau_{cd}}))$$

and c_b is the near-bed suspended-sediment concentration for the grainsize at hand.

MIKE3 FM MT gives two choices for determining c_b : the Teeter formulation and the Rouse formulation. The Teeter formulation was chosen for implementation here, which is:

$$c_b = \bar{c} \left(1 + \frac{p_e}{1.25 + 4.75 p_d^{2.5}} \right)$$

where p_e is the Peclet number, defined as:

$$p_e = 6 \frac{w_s}{\kappa U_f}$$

and U_f is the friction velocity.

The calibration process involves selecting the fall velocity and the critical bed shear stress for deposition (τ_{cd}) for each grainsize.

8.4.2 Erosion

Erosion of bed material takes place when and where the bed shear stress exceeds the critical shear stress for erosion (τ_{ce}). A single value of τ_{ce} is assigned for the bed sediment as a whole.

The erosion rate (kg/[m²s]) is specified for the bed as a whole as:

$$E = E_I \exp(\alpha(\tau_b - \tau_{ce}))$$

where α is a power term and E_I is the "initial" erosion rate. The total mass of sediment eroded from the bed (which is governed by E) is then distributed amongst the constituent grainsizes by the proportions of the constituent grainsizes in the bed sediment. For example, if constituent grainsize #1 makes up 50% of the bed sediment by mass then 50% of the sediment eroded by E will be assigned that grainsize. The calibration process involves selecting one value each for τ_{ce} , α and E_I .

Table A1:

List of specific calibration parameters and calibrated as implemented in the DHI MIKE3 FM HD and MT model for Okura Estuary and Karepiro Bay.

DHI MIKE3 FM	Parameter	Variable used in model
Model stability	Model Spin up Time	10 days
Offshore tidal boundary	Harmonic Tidal constituents	M ₂ , S ₂ , N ₂
Bed roughness	Z ₀	0.05
Horizontal Mixing	Smagorinsky coefficient	0.28
Lower limit	N _(x,y)	1.8e-006 m ² /s
Upper limit	N _(x,y)	10 m ² /s
Vertical Mixing	C _μ	0.09
k-ε formulation	C1 _ε	1.44
	C2 _ε	1.92
	C3 _ε	0
	σ _t	0.9
	σ _k	1
	σ _ε	1.3
Salinity scaling factor	S	1.1
Wind drag coefficient	C _d	0.00125
Particle Settling Velocity	15μm	1.3e-4 m/s
Bed Erosion Rate	E1	6e-5 kg/m ² /s
	α	4.3
Sediment Deposition Threshold	τ _{od} (15μm)	0.1 N/m ²

9 Appendix 2: LIDAR data processing

The LIDAR data were supplied to NIWA in a raster (*.las) format, which, once imported into LASEdit software can be viewed, post processed and output into an *.xyz (ascii readable format). These data were then converted from NZTM, corrected to local chart datum and converted to WGS84 co-ordinates and saved in a binary Matlab format for further post processing.

Several hundred binary files were then put through a data reduction routine to make the size of data importable to the DHI MIKE ZERO grid generation tool. Each data file (tile) was concatenated and interpolated onto a regular grid of a sub-region of the area. Then each sub-region was concatenated again and interpolated onto a regular grid of the whole region. In this way LIDAR bathymetry can easily be reprocessed using Matlab files if higher/lower spatial resolution is required.